

# Impact of acetone on ozone production and OH in the upper troposphere at high $\text{NO}_x$

Ian Folkins

Atmospheric Science Program, Departments of Physics and Oceanography, Dalhousie University  
Halifax, Nova Scotia, Canada

Robert Chatfield

Earth Science Division, NASA Ames Research Center, Moffett Field, California

**Abstract.** The impact of acetone (or any  $\text{HO}_x$  source) on tropospheric photochemistry is largest in the high  $\text{NO}_x$  regime. The fractional increases in OH and ozone production associated with acetone increase rapidly with  $\text{NO}_x$  when  $\text{NO}_x$  mixing ratios become larger than 300 parts per trillion by volume (pptv). This occurs in part because the  $\text{HO}_x$  yield of acetone is larger at higher  $\text{NO}_x$  mixing ratios, going from about 1  $\text{HO}_x$  at  $\text{NO}_x \sim 10$  pptv to 3  $\text{HO}_x$  at  $\text{NO}_x \sim 1000$  pptv. We also investigate the effect of acetone on the partitioning of the  $\text{NO}_y$  family. Acetone increases the conversion of NO to  $\text{NO}_2$ ,  $\text{HNO}_4$ ,  $\text{HNO}_3$ , and peroxyacetyl nitrate (PAN). Conversion of NO to PAN dominates at low  $\text{NO}_x$ , while conversion of NO to  $\text{HNO}_3$  dominates at high  $\text{NO}_x$ . These NO decreases significantly diminish the increases in OH and ozone production one would otherwise anticipate from the increases in  $\text{HO}_2$ . In particular, acetone can be expected to reduce ozone production for  $\text{NO}_x < 25$  pptv. We also show that most of the changes in species concentrations arising from the introduction of a  $\text{HO}_x$  source can be accurately predicted using simple expressions derived from linear perturbation theory.

## 1. Introduction

The main source of  $\text{HO}_x$  ( $= \text{OH} + \text{HO}_2$ ) in the troposphere is the reaction of  $\text{O}^1\text{D}$  with  $\text{H}_2\text{O}$ , which produces two OH radicals. This source decreases with height due to the rapid decrease of water vapor number densities with altitude. The weakness of this  $\text{HO}_x$  source in the upper troposphere provides an opportunity for a number of other species to make significant contributions to  $\text{HO}_x$  production in this region. In particular, there are several chemical species that, although chemically produced near the surface, can be transported into the upper troposphere by deep convection or synoptic systems and which subsequently photolyze to produce  $\text{HO}_x$ . These  $\text{HO}_x$  precursors include acetone ( $\text{CH}_3\text{COCH}_3$ ), methyl hydroperoxide ( $\text{CH}_3\text{OOH}$ ), and possibly formaldehyde ( $\text{CH}_2\text{O}$ ).

The vertical transport of  $\text{HO}_x$  precursors to the upper troposphere [Chatfield and Crutzen, 1984] has gained more attention recently due to, among other factors, the realization that acetone is a  $\text{HO}_x$  source and that its concentration can be quite high in the upper troposphere [Singh *et al.*, 1995; Arnold *et al.*, 1997], that per-

oxide concentrations in the upper tropical troposphere are much higher than can be explained by steady state models [Jacob *et al.*, 1996; Jaeglé *et al.*, 1997], and the fact that instruments capable of measuring OH and  $\text{HO}_2$  in the upper troposphere have been developed and there has been a concerted effort to account for their observed concentrations [Wennberg *et al.*, 1998]. These  $\text{HO}_x$  sources affect upper tropospheric chemistry in a number of different ways. First, they increase the oxidizing power of the atmosphere by directly increasing OH and  $\text{HO}_2$ . Second, the higher  $\text{HO}_2$  concentrations increase ozone production from the  $\text{NO} + \text{HO}_2$  reaction [Prather and Jacob, 1997; Folkins *et al.*, 1997; Wennberg *et al.*, 1998; Folkins *et al.*, 1998; Jaeglé *et al.*, 1998]. Third, they affect  $\text{NO}_y$  partitioning by increasing the rate at which  $\text{NO}_x$  is oxidized to  $\text{HNO}_3$  and  $\text{HNO}_4$ , and in the case of acetone, also to peroxyacetyl nitrate (PAN) [McKeen *et al.*, 1997; Keim *et al.*, 1999]. These  $\text{NO}_x$  decreases offset, to some extent, the increases in ozone production associated with the increases in  $\text{HO}_2$ . This effect has been examined using a three-dimensional model [Müller and Brasseur, 1999].

We examine how the effects of adding acetone to the upper troposphere depend on  $\text{NO}_x$ . There are several reasons for anticipating that such a dependence might exist. First, the number of  $\text{HO}_x$  produced during the oxidation of acetone, or any hydrocarbon, should increase with  $\text{NO}_x$ . Second, while the dominant  $\text{HO}_x$  loss

Copyright 2000 by the American Geophysical Union.

Paper number 2000JD900067.  
0148-0227/00/2000JD900067\$09.00

processes at low NO<sub>x</sub> involve reactions between HO<sub>x</sub> species (e.g., OH+HO<sub>2</sub> and HO<sub>2</sub>+HO<sub>2</sub>), the dominant HO<sub>x</sub> loss process at high NO<sub>x</sub> (OH+NO<sub>2</sub>) is linear in HO<sub>x</sub>. This should give rise to some change in the response of HO<sub>x</sub> to additional HO<sub>x</sub> sources. Finally, the response of HO<sub>x</sub> to acetone will be proportional in some sense to the fractional contribution of acetone to the total HO<sub>x</sub> production. One of the most important sources of HO<sub>x</sub> to the upper troposphere is methane (CH<sub>4</sub>) oxidation. This source starts to diminish at high NO<sub>x</sub> as OH becomes small, which will increase the relative importance of acetone oxidation to the total HO<sub>x</sub> production.

We first introduce a zero-dimensional (point) photochemical model intended to approximate the upper tropical troposphere. (Acetone is also an important HO<sub>x</sub> source to the midlatitude upper troposphere, but it is important over a much broader altitude range in the tropics.) There is a prescribed input of convected air into the model each day, and it is run until there is an approximate steady state between the convective forcing and in situ chemistry. After describing some of the baseline chemical characteristics of this model, we introduce acetone into the convected air and examine the resulting fractional changes in OH, HO<sub>2</sub>, NO, and NO<sub>2</sub>. We show how standard steady state expressions for the partitioning of the HO<sub>x</sub> and NO<sub>x</sub> families can be used to estimate the fractional changes in these species. We then analyze the HO<sub>x</sub> budget to show why the largest fractional changes in OH and HO<sub>2</sub> occur at high NO<sub>x</sub>. This analysis requires some method for estimating the HO<sub>x</sub> yields of acetone and methane, i.e., the number of HO<sub>x</sub> produced by each of these hydrocarbons as they oxidize. It is usually very difficult to calculate HO<sub>x</sub> yields of hydrocarbons directly from numerical simulations. We therefore describe a procedure by which the HO<sub>x</sub> yields of methane and acetone might be estimated analytically.

The second part of this paper deals with the impact of acetone on ozone production. Acetone increases ozone production by increasing the concentration of HO<sub>2</sub>. This is offset by decreases in ozone production associated with the conversion of NO to NO<sub>2</sub>, HNO<sub>4</sub>, HNO<sub>3</sub>, and PAN. We first derive expressions which predict the enhancements in PAN, HNO<sub>3</sub>, and HNO<sub>4</sub> associated with the introduction of acetone. These expressions assume that acetone simply moves the concentration of each species from one photochemical steady state to another and that the fractional change in each species is small. After determining how these changes effect NO, we estimate the net impact of acetone on ozone production.

## 2. Photochemical Model

As was mentioned earlier, the photochemical model is designed to strike a realistic balance in the upper tropical troposphere between the two forcings of convective

input and in situ chemistry. It is a modified version of a zero-dimensional photochemical model used in previous studies [Chatfield *et al.*, 1996; Folkins *et al.*, 1998]. The air parcel is at 10 km, near the altitude of maximum convective outflow. The effect of acetone will increase with height from 10 km toward the tropical tropopause. The temperature is 227 K, the water vapor mixing ratio is 100 ppmv, and the surface albedo is 0.1. The effect of convective detrainment is modeled using a replacement time of 15 days. Over the course of a day, the concentration of each species is fractionally reduced by an amount equal to 1/15 and increased by an amount depending on the prescribed properties of convected air. This replacement rate is consistent with those derived from a three-dimensional model [Prather and Jacob, 1997]. The model was run until a reasonable steady state balance between convection and in situ chemistry is achieved (here 50 days). The incoming convected air had CO = 60 ppbv, O<sub>3</sub> = 20 ppbv, CH<sub>4</sub> = 1.7 ppmv, and H<sub>2</sub>O<sub>2</sub> = CH<sub>3</sub>OOH = 50 parts per trillion by volume (pptv), while the concentrations of NO<sub>2</sub>, NO<sub>3</sub>, N<sub>2</sub>O<sub>5</sub>, HNO<sub>4</sub>, HNO<sub>3</sub>, CH<sub>2</sub>O, and PAN were all set to zero. The NO mixing ratio of the incoming convected air was varied from 10 to 6000 pptv. Two runs were done for each value of the incoming NO mixing ratio. In the baseline runs, the acetone mixing ratio was set equal to zero, while in the perturbation runs it was set equal to 600 pptv.

Figure 1 gives some indication of the chemical properties of the baseline run. In the lower panel day-averaged HO<sub>2</sub>, OH, and O<sub>3</sub> mixing ratios are plotted against the ambient NO<sub>x</sub> mixing ratio. The ambient NO<sub>x</sub> mixing ratio was less than the NO<sub>x</sub> mixing ratio of the incoming convected air because of the conversion, in the model, of NO to other NO<sub>y</sub> species.

The upper panel of Figure 1 shows diurnally averaged ozone production rates in the model. The net rate of ozone production in the background troposphere can be written

$$d[\text{O}_3]/dt = P(\text{O}_3) - D(\text{O}_3), \quad (1)$$

where

$$P(\text{O}_3) = k_6[\text{NO}][\text{HO}_2] + k_{10}[\text{NO}][\text{CH}_3\text{O}_2] \quad (2)$$

$$D(\text{O}_3) = k_{11}[\text{O}^1D][\text{H}_2\text{O}] + k_7[\text{OH}][\text{O}_3] + k_5[\text{HO}_2][\text{O}_3]. \quad (3)$$

Each of these five terms has been plotted against NO<sub>x</sub> in the top panel of Figure 1. The largest of the five terms is HO<sub>2</sub>+NO (dashed line), which is almost equal to the total  $d\text{O}_3/dt$  (bold solid line) at all NO<sub>x</sub> mixing ratios.

The upper panel of Figure 2 shows the acetone mixing ratio in the model when 600 pptv of acetone is added to the incoming convected air. The resulting ambient acetone mixing ratios of between 290 and 320 pptv are roughly consistent with observed upper tropical tro-

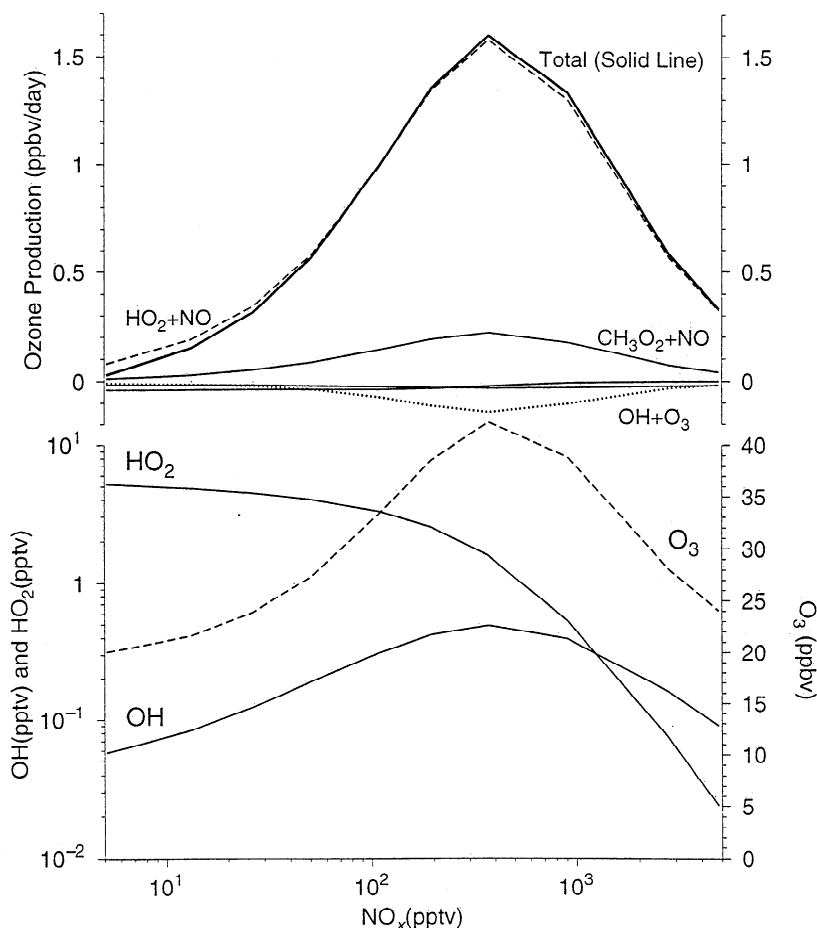


**Figure 1.** (bottom) Mixing ratios of OH in parts per trillion by volume (pptv), HO<sub>2</sub> (pptv), and O<sub>3</sub> (ppbv) in the baseline model run plotted against NO<sub>x</sub>. (top) Ozone production and destruction terms in the baseline model run plotted against NO<sub>x</sub>. The two small unlabeled ozone destruction terms are OH + O<sub>3</sub> and O<sup>1</sup>D + H<sub>2</sub>O. The dashed line represents ozone production from the HO<sub>2</sub> + NO reaction. The dotted line represents destruction from the HO<sub>2</sub> + O<sub>3</sub> reaction. The bold line represents the sum of all five production and destruction terms.

ospheric mixing ratios of between 200 and 450 pptv [Singh *et al.*, 1995]. Although the main sink of acetone in the model is photolysis, OH attack is significant in the range of NO<sub>x</sub> mixing ratios at which OH concentrations are largest.

The upper panel of Figure 2 also shows the fractional change of O<sub>3</sub> in going from the baseline to the perturbed simulation (i.e.,  $dO_3/O_3 = (O_3(\text{acetone}) - O_3(\text{baseline}))/O_3(\text{baseline})$ ). In contrast to the O<sub>3</sub> mixing ratio,  $dO_3/O_3$  is an increasing function of NO<sub>x</sub>.

The lower panel of Figure 2 shows the fractional changes in OH, HO<sub>2</sub>, NO, and NO<sub>2</sub> that are associated with the introduction of acetone. The fractional reductions in NO and NO<sub>2</sub> are largest at low NO<sub>x</sub>, while the increases in OH and HO<sub>2</sub> increase rapidly with NO<sub>x</sub> for NO<sub>x</sub> larger than 300 pptv.

### 3. HO<sub>x</sub> and NO<sub>x</sub> Partitioning

The lower panel of Figure 2 shows that acetone favors the partitioning of HO<sub>x</sub> to HO<sub>2</sub> and of NO<sub>x</sub> to NO<sub>2</sub>.

This can be explained using the standard steady state expressions for the partitioning of HO<sub>x</sub> and NO<sub>x</sub>. Using the reaction labeling convention given in Appendix A, the OH/HO<sub>2</sub> ratio is approximately given by

$$\frac{[\text{OH}]}{[\text{HO}_2]} = \frac{k_5[\text{O}_3] + k_6[\text{NO}]}{k_7[\text{O}_3] + k_8[\text{CO}]} \quad (4)$$

If the fractional changes in OH, HO<sub>2</sub>, and NO are small, and it is assumed that the fractional changes in CO and O<sub>3</sub> associated with the introduction of acetone can be ignored, it can be shown that

$$\frac{d\text{OH}}{\text{OH}} = \frac{d\text{HO}_2}{\text{HO}_2} + f_{19} \frac{d\text{NO}}{\text{NO}} \quad (5)$$

The fractional reaction rate  $f_{19}$  is defined in Appendix B as the relative likelihood that an HO<sub>2</sub> radical will react with NO as opposed to either NO or O<sub>3</sub>. Its dependence on NO<sub>x</sub> is shown in Figure 3.

The lower panel of Figure 4 compares  $d\text{OH}/\text{OH}$  in the model with the estimate given in (5). The agree-

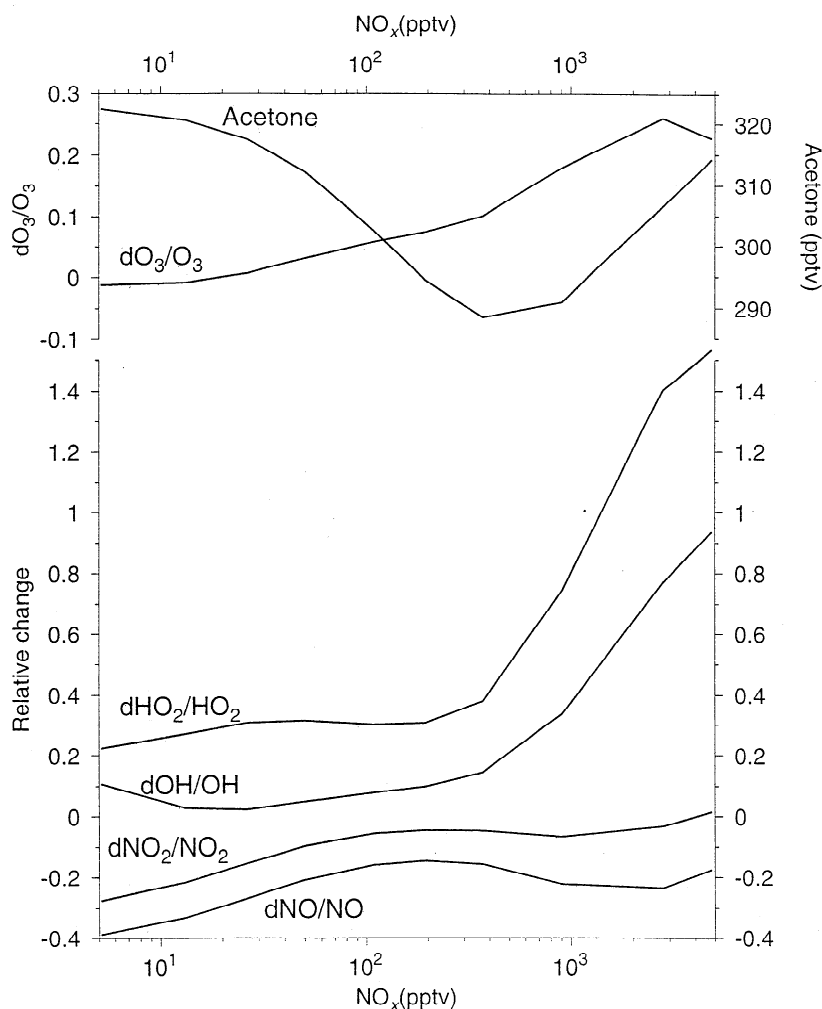


**Figure 2.** (bottom) Fractional changes in OH, HO<sub>2</sub>, NO, and NO<sub>2</sub> from the baseline model run associated with the introduction of acetone into the model. (top) Fractional change in O<sub>3</sub> (ppbv) caused by the addition of acetone. Also shown is the acetone mixing ratio (pptv) in the model.

ment is quite good at low NO<sub>x</sub>. The negative contribution of the  $d\text{NO}/\text{NO}$  term in (5) lowers  $d\text{HO}_2/\text{HO}_2$  and brings the predicted  $d\text{OH}/\text{OH}$  closer to the modeled value. The agreement is poor at high NO<sub>x</sub>.

The top panel of Figure 2 shows that  $d\text{O}_3/\text{O}_3$  is not necessarily small. However, the variation of O<sub>3</sub> can be neglected in (5) because the fractional reaction rates that couple  $d\text{OH}/\text{OH}$  to  $d\text{O}_3/\text{O}_3$  are small unless NO<sub>x</sub> mixing ratios are extremely low, in which case  $d\text{O}_3/\text{O}_3$  is small.

The standard expression for partitioning NO<sub>x</sub> is

$$\frac{\text{NO}}{\text{NO}_2} = \frac{J_{\text{NO}_2}}{k_9[\text{O}_3] + k_6[\text{HO}_2]} \quad (6)$$

This yields a first-order relationship between  $d\text{NO}$  and  $d\text{NO}_2$  given by

$$\frac{d\text{NO}_2}{\text{NO}_2} = \frac{d\text{NO}}{\text{NO}} + f_{18} \frac{d\text{HO}_2}{\text{HO}_2} + (1 - f_{18}) \frac{d\text{O}_3}{\text{O}_3} \quad (7)$$

NO<sub>2</sub> is coupled to changes in HO<sub>2</sub> and O<sub>3</sub> via the fractional reaction rate  $f_{18}$ . The coupling of NO<sub>2</sub> to HO<sub>2</sub>

is strongest at low NO<sub>x</sub> where  $f_{18}$  is large (see Figure 3). NO<sub>2</sub> is most sensitive to changes in O<sub>3</sub> at high NO<sub>x</sub>, where  $(1 - f_{18})$  is largest. The upper panel of Figure 4 compares the change in NO<sub>2</sub> predicted by (7) with the actual change of NO<sub>2</sub> in the model. Neglect of the  $d\text{O}_3/\text{O}_3$  term in (7) would lead to substantial disagreement with modeled  $d\text{NO}_2/\text{NO}_2$  at high NO<sub>x</sub>. The full expression agrees quite well with  $d\text{NO}_2/\text{NO}_2$  over the entire range of NO<sub>x</sub> mixing ratios.

#### 4. HO<sub>x</sub> Budget

Steady state expressions for the partitioning of HO<sub>x</sub> and NO<sub>x</sub> are of some help in interrelating some of the changes in HO<sub>x</sub> and NO<sub>x</sub> caused by the introduction of HO<sub>x</sub> sources. However, they cannot be used to predict the absolute response of HO<sub>x</sub> to a HO<sub>x</sub> source. This requires an analysis of the HO<sub>x</sub> budget. The three most pervasive sources of HO<sub>x</sub> to the upper troposphere are the O<sup>1</sup>D + H<sub>2</sub>O reaction, methane oxidation, and acetone oxidation. Quantifying the size of the O<sup>1</sup>D + H<sub>2</sub>O source is straightforward. However, both methane

and acetone have a large number of oxidation pathways, each of which will produce or destroy different numbers of HO<sub>x</sub>. In a computer simulation it is difficult to determine from which hydrocarbon a HO<sub>x</sub> originates because the oxidation pathways of methane and acetone have many intermediates in common. We show in Appendices C and D how a modified version of a previously introduced method [Arnold *et al.*, 1997] can be used to predict the HO<sub>x</sub> yields of methane, acetone and their intermediates.

The HO<sub>x</sub> yields of CH<sub>3</sub>OOH and methane, calculated using the fractional reaction rates from the model and the expressions given in Appendix C, are plotted against the ambient NO<sub>x</sub> mixing ratio in Figure 5. The HO<sub>x</sub> yield of CH<sub>3</sub>OOH is anticorrelated with the OH mixing ratio and varies between 1 and 2. Within the usual range of NO<sub>x</sub> mixing ratios in the upper troposphere (10 pptv ≤ NO<sub>x</sub> ≤ 100 pptv), it can be considered a decreasing function of NO<sub>x</sub>. The HO<sub>x</sub> yield of methane slowly increases with NO<sub>x</sub> [see also Müller and Brasseur, 1999].

The HO<sub>x</sub> yield of acetone was calculated using the method of Appendix D and is plotted against NO<sub>x</sub> in Figure 5. It increases rapidly from 0.5 at NO<sub>x</sub> = 5 pptv to 2.5 at NO<sub>x</sub> = 1000 pptv. Also shown is the HO<sub>x</sub> yield

of acetone assuming the only sink is photolysis. Consideration of the OH channel significantly reduces the HO<sub>x</sub> yield of acetone in the intermediate range of NO<sub>x</sub> mixing ratios for which OH concentrations are largest. Singh *et al.* [1995] have demonstrated that the HO<sub>x</sub> yield of acetone via the photolysis channel is 3.2 in the high NO<sub>x</sub> limit. This approximation is quite accurate for NO<sub>x</sub> ≥ 100 pptv but significantly overestimates HO<sub>x</sub> production from acetone for much of the observed range of NO<sub>x</sub> mixing ratios in the upper troposphere [see also Müller and Brasseur, 1999].

The three main sources of HO<sub>x</sub> in the model have been plotted against NO<sub>x</sub> in Figure 6. The production of HO<sub>x</sub> from methane oxidation (PHO<sub>x</sub>(CH<sub>4</sub>)) and from acetone oxidation (PHO<sub>x</sub>(ACET)) have been calculated using (C1) and (D1). The dependence of PHO<sub>x</sub>(CH<sub>4</sub>) on NO<sub>x</sub> arises mainly from its dependence on [OH]. The variation in PHO<sub>x</sub>(O<sup>1</sup>D+H<sub>2</sub>O) with NO<sub>x</sub> reflects its dependence on [O<sub>3</sub>]. The increase in PHO<sub>x</sub>(ACET) with NO<sub>x</sub> occurs largely because the HO<sub>x</sub> yield of acetone is an increasing function of NO<sub>x</sub>. Also plotted in Figure 6 are LHO<sub>x</sub>(OH+HO<sub>2</sub>) and LHO<sub>x</sub>(OH+NO<sub>2</sub>), the dominant HO<sub>x</sub> sinks at low and high NO<sub>x</sub>, respectively. Not all HO<sub>x</sub> sinks are shown. Formation of H<sub>2</sub>O<sub>2</sub> is the second most impor-

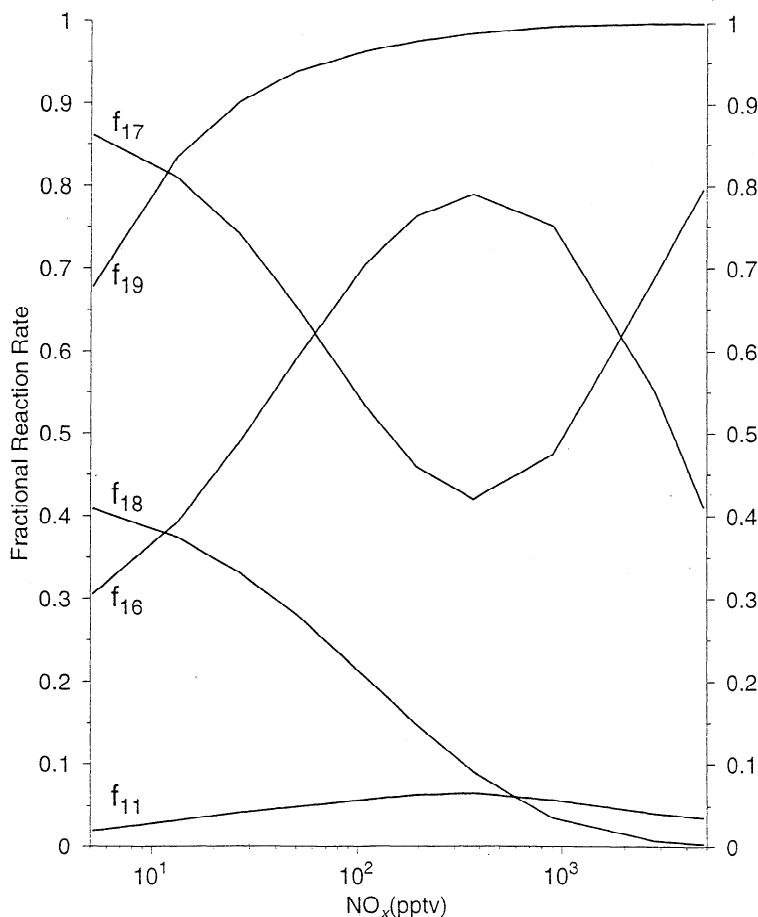


**Figure 3.** The dependence against NO<sub>x</sub> of five fractional reaction rates: f<sub>17</sub>, fraction of HNO<sub>3</sub> undergoing photolysis; f<sub>19</sub>, fraction of HO<sub>2</sub> reacting with NO; f<sub>18</sub>, fraction of NO reacting with HO<sub>2</sub>; f<sub>16</sub>, fraction of HNO<sub>4</sub> reacting with OH; and f<sub>11</sub>, fraction of CH<sub>3</sub>COO<sub>2</sub> reacting with NO<sub>2</sub>.

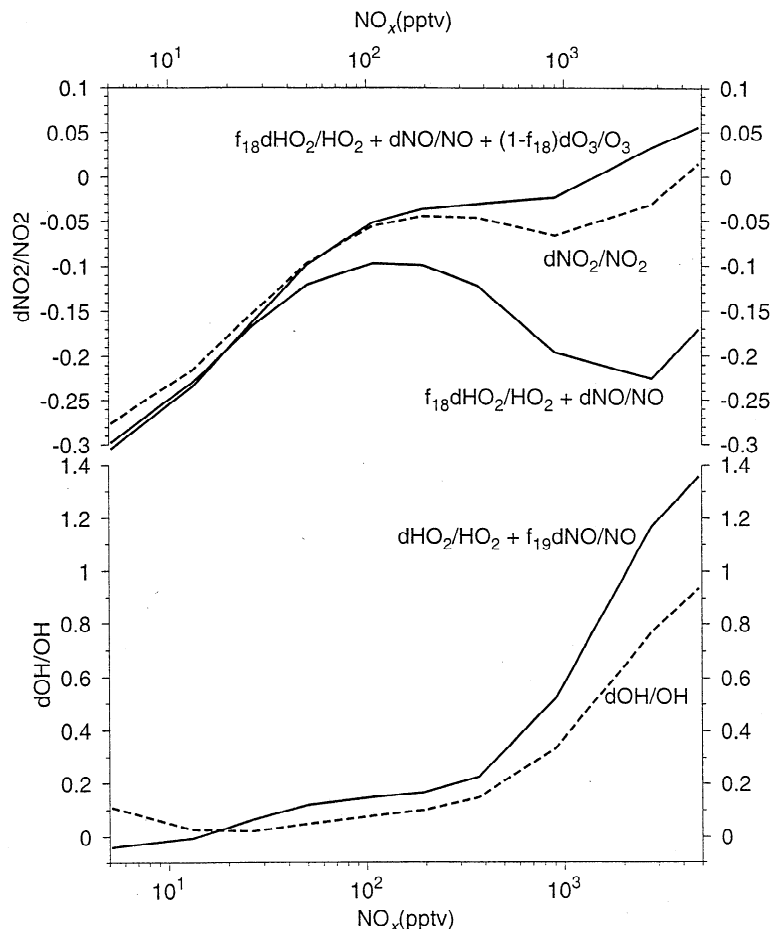


**Figure 4.** (bottom) The fractional change in OH from the introduction of acetone into the model compared with the change predicted by equation (5). (top) The fractional change in NO<sub>2</sub> from the introduction of acetone into the model compared with the change predicted by (7), with and without the contribution from the ozone response. The change in ozone has a strong effect on the change in NO<sub>2</sub> at high NO<sub>x</sub>.

tant HO<sub>x</sub> at low NO<sub>x</sub>, where HO<sub>2</sub> concentrations are high. Formation of HNO<sub>4</sub> is important in an intermediate range of NO<sub>x</sub> concentrations but goes to zero in both the low and high NO<sub>x</sub> limits.

The complexity of the HO<sub>x</sub> budget makes it difficult to predict the response of HO<sub>x</sub> to acetone over the entire range of NO<sub>x</sub> mixing ratios. We determine this response in the low and high NO<sub>x</sub> limits. If there is no net change in HO<sub>x</sub> over a day,

$$\text{LHO}_x = \text{PHO}_x. \quad (8)$$

In the absence of acetone and in the low NO<sub>x</sub> limit,

$$\begin{aligned} k_{\text{OH}+\text{HO}_2}[\text{OH}][\text{HO}_2] = \\ \text{PHO}_x(\text{O}^1\text{D} + \text{H}_2\text{O}) + \text{PHO}_x(\text{CH}_4). \end{aligned} \quad (9)$$

The presence of acetone will introduce increases in PHO<sub>x</sub>(O<sup>1</sup>D) that scale with dO<sub>3</sub>/O<sub>3</sub> and increases in PHO<sub>x</sub>(CH<sub>4</sub>) that scale with dOH/OH. We assume that these changes in the HO<sub>x</sub> budget are small compared with PHO<sub>x</sub>(ACET). In that case,

$$\begin{aligned} k_{\text{OH}+\text{HO}_2}[\text{OH} + d\text{OH}][\text{HO}_2 + d\text{HO}_2] = \\ \text{PHO}_x + \text{PHO}_x(\text{ACET}). \end{aligned} \quad (10)$$

To first order in dOH and dHO<sub>2</sub>, this gives under low NO<sub>x</sub>

$$\frac{d\text{OH}}{\text{OH}} + \frac{d\text{HO}_2}{\text{HO}_2} = \frac{\text{PHO}_x(\text{ACET})}{\text{PHO}_x}. \quad (11)$$

The right- and left-hand sides of (11) have been plotted against NO<sub>x</sub> in Figure 7. There is reasonable agreement at low NO<sub>x</sub>. Equation (11) gives some insight into why the impact of acetone on OH in the low NO<sub>x</sub> limit is smaller than what one might anticipate. First, dOH/OH is small because the production of HO<sub>x</sub> from acetone, normalized by the total unperturbed HO<sub>x</sub> production, is constrained to equal the sum dOH/OH + dHO<sub>2</sub>/HO<sub>2</sub>. Second, changes in HO<sub>x</sub> partitioning arising from changes in NO constrain dHO<sub>2</sub>/HO<sub>2</sub> to be larger than dOH/OH, which by (11) must reduce dOH/OH. Third, the HO<sub>x</sub> yield of acetone is small at low NO<sub>x</sub>.

A similar analysis can also be carried out in the high NO<sub>x</sub> limit. Assume in the absence of acetone that

$$k_{\text{OH}+\text{NO}_2}[\text{OH}][\text{NO}_2] = \text{PHO}_x(\text{O}^1\text{D} + \text{H}_2\text{O}) + \text{PHO}_x(\text{CH}_4). \quad (12)$$

Acetone will then induce changes in OH and NO<sub>2</sub> such that

$$\frac{d\text{OH}}{\text{OH}} + \frac{d\text{NO}_2}{\text{NO}_2} = \frac{\text{PHO}_x(\text{ACET})}{\text{PHO}_x}. \quad (13)$$

Figure 7 shows that there is excellent agreement between the two sides of this equation for NO<sub>x</sub> ≥ 800 pptv. In this limit, OH is quite sensitive to the introduction of acetone. This is partly because  $d\text{NO}_2/\text{NO}_2$  is very small, so that  $d\text{OH}/\text{OH}$  is roughly equal to  $\text{PHO}_x(\text{ACET})/\text{PHO}_x$ . The fractional contribution of acetone to the total HO<sub>x</sub> production itself also increases with NO<sub>x</sub>. This is because the HO<sub>x</sub> yield of acetone increases with NO<sub>x</sub> and because decreases in OH and O<sub>3</sub> at high NO<sub>x</sub> reduce PHO<sub>x</sub>.

## 5. Ozone Production

The five largest ozone production and destruction terms in the model were shown in Figure 1. The NO

+ HO<sub>2</sub> term is larger than the other four by about an order of magnitude. We will assume that most of the changes in ozone production from a HO<sub>x</sub> source arise from changes in this term. The fractional change in P(O<sub>3</sub>) associated with the introduction of a HO<sub>x</sub> source can then be approximated as

$$\frac{dP(\text{O}_3)}{P(\text{O}_3)} = \frac{d\text{HO}_2}{\text{HO}_2} + \frac{d\text{NO}}{\text{NO}}. \quad (14)$$

The validity of this approximation is assessed in Figure 8. The two sides of (14) agree well for NO<sub>x</sub> ≤ 300 pptv. They start to differ at high NO<sub>x</sub> because the increasing magnitude of  $d\text{HO}_2/\text{HO}_2$  undermines the validity of the linearized approach.

In the absence of changes in NO, the fractional change in P(O<sub>3</sub>) would equal the fractional change in HO<sub>2</sub>. Figure 8 shows that  $dP(\text{O}_3)/P(\text{O}_3)$  is substantially smaller than  $d\text{HO}_2/\text{HO}_2$ , especially when NO<sub>x</sub> mixing ratios are less than 300 pptv. When NO<sub>x</sub> is less than 25 pptv, the NO reduction is larger than the HO<sub>2</sub> increase, so that acetone gives rise to a net decrease in ozone production.

Perturbation theory can be used to help predict the response of P(O<sub>3</sub>) to a HO<sub>x</sub> source if  $d\text{NO}/\text{NO}$  can be expressed in terms of  $d\text{HO}_2/\text{HO}_2$ . To do this, we

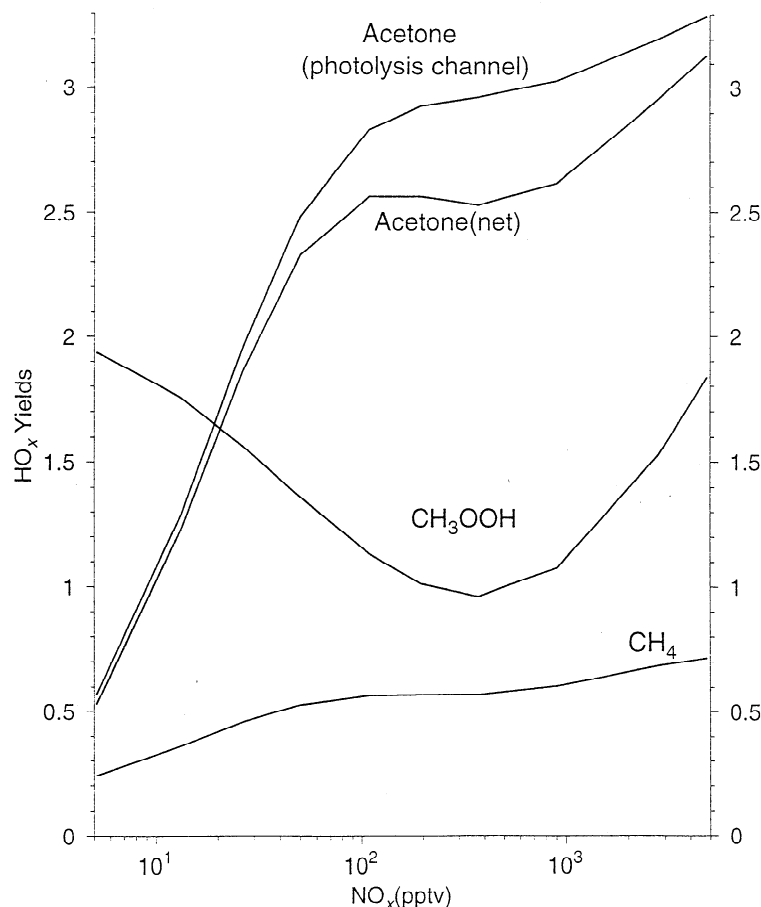


**Figure 5.** The HO<sub>x</sub> yields of methane (CH<sub>4</sub>), methyl hydroperoxide (CH<sub>3</sub>OOH), acetone (OH attack and photolysis channels), and acetone (photolysis channel only), plotted against NO<sub>x</sub>.

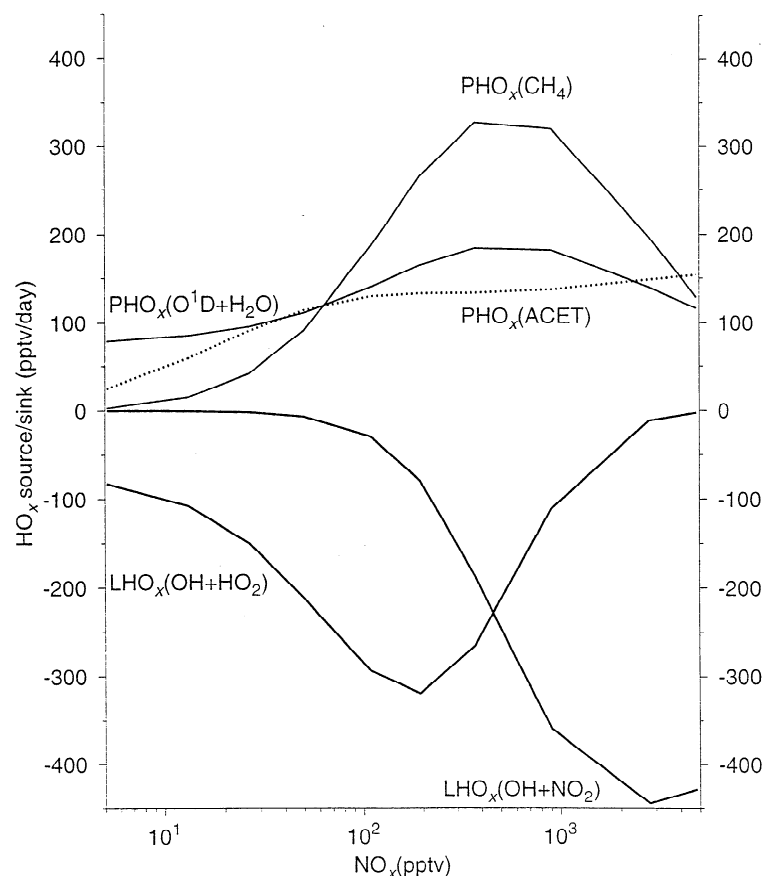


**Figure 6.** The dominant HO<sub>x</sub> sources and sinks in the model plotted against NO<sub>x</sub>. Each rate is a day average. PHO<sub>x</sub>(ACET) is represented by the dotted line.

assume that the introduction of acetone results in an increased conversion of NO to NO<sub>2</sub>, HNO<sub>4</sub>, HNO<sub>3</sub>, and PAN but to no other NO<sub>y</sub> species.

$$\text{NO} \frac{d\text{NO}}{\text{NO}} + \text{NO}_2 \frac{d\text{NO}_2}{\text{NO}_2} + \text{HNO}_4 \frac{d\text{HNO}_4}{\text{HNO}_4} + \text{HNO}_3 \frac{d\text{HNO}_3}{\text{HNO}_3} + d\text{PAN} = 0. \quad (15)$$

This expression implicitly assumes that the introduction of a HO<sub>x</sub> source has no effect on the NO<sub>y</sub> lifetime. The response of NO<sub>2</sub> to a HO<sub>x</sub> source is given in (7). Those of HNO<sub>4</sub>, HNO<sub>3</sub>, and PAN can be obtained by again using the assumption of photochemical steady state.

The thermal decomposition of HNO<sub>4</sub> can be ignored in the upper troposphere. If the sources and sinks of HNO<sub>4</sub> are those given in Appendix A, it can be shown that

$$\frac{d\text{HNO}_4}{\text{HNO}_4} = \frac{d\text{NO}_2}{\text{NO}_2} + \frac{d\text{HO}_2}{\text{HO}_2} - f_{16} \frac{d\text{OH}}{\text{OH}}. \quad (16)$$

The fractional reaction rate  $f_{16}$  is defined in Appendix B. Its variation with NO<sub>x</sub> is shown in Figure 3. The fractional change in HNO<sub>4</sub> predicted by (16) is compared with the actual fractional change of HNO<sub>4</sub> in the lower panel of Figure 9. The agreement is quite good.

If the sources and sinks of HNO<sub>3</sub> are those listed in Appendix B, then the change in HNO<sub>3</sub> can be approximated as

$$\frac{d\text{HNO}_3}{\text{HNO}_3} = \frac{d\text{NO}_2}{\text{NO}_2} + f_{17} \frac{d\text{OH}}{\text{OH}}, \quad (17)$$

where  $f_{17}$  is defined in Appendix B and plotted versus NO<sub>x</sub> in Figure 3. The middle panel of Figure 9 compares the fractional change in HNO<sub>3</sub> predicted by (17) with the change in the model. The agreement is again very good, despite the long photochemical lifetime of HNO<sub>3</sub>. Acetone reduces HNO<sub>3</sub> for NO<sub>x</sub> less than 100 pptv, where the decrease in  $d\text{NO}_2/\text{NO}_2$  more than offsets the increase in  $d\text{OH}/\text{OH}$ .

PAN is formed by the reaction between CH<sub>3</sub>COO<sub>2</sub> and NO<sub>2</sub>. The dominant source of CH<sub>3</sub>COO<sub>2</sub> in the model is acetone photolysis. The dominant sink of PAN in the model is photolysis. At steady state,

$$f_{11} J_{\text{ACET}}[\text{ACET}] = J_{\text{PAN}}[\text{PAN}]. \quad (18)$$

In this expression,  $f_{11}$  represents the fractional reaction rate for the conversion of CH<sub>3</sub>COO<sub>2</sub> to PAN. As is shown in Figure 3, this rate varies between 0.02 and 0.07 (i.e., 2-7% efficiency for the conversion of acetone to PAN). Since [PAN] = 0 in the baseline run, [PAN] = [dPAN], and

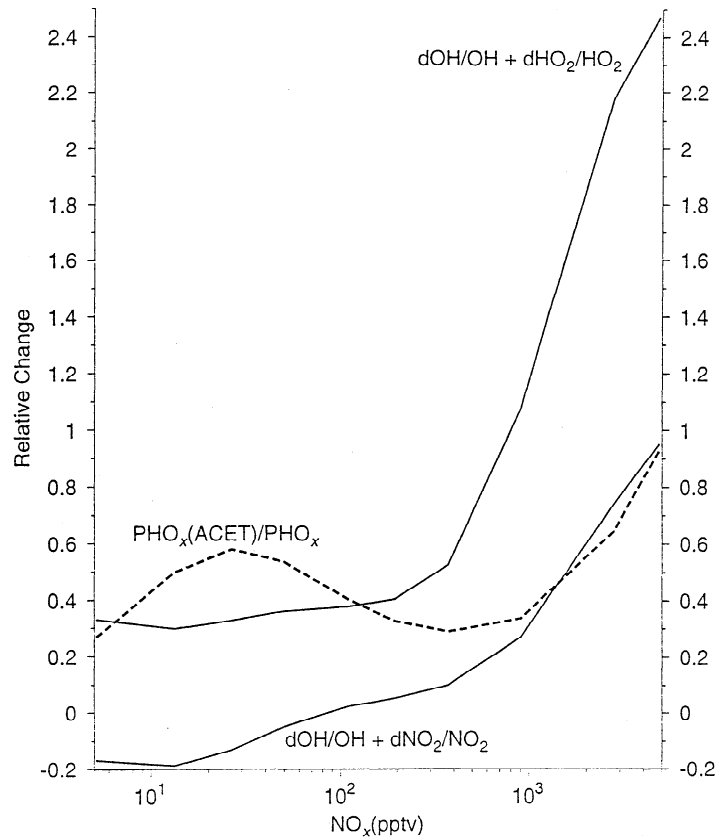


**Figure 7.** The dotted line represents the production of HO<sub>x</sub> from acetone, normalized by the total production of HO<sub>x</sub> in the baseline model. The two solid lines represent the sum of the fractional changes in OH and HO<sub>2</sub> and in OH and NO<sub>2</sub>.

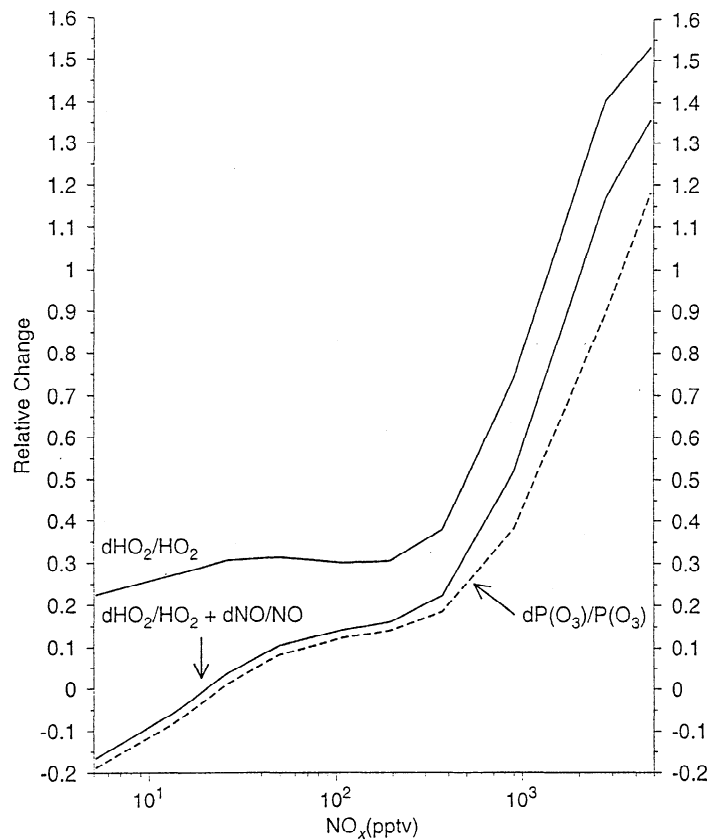


**Figure 8.** The fractional change in ozone production from adding acetone to the model (dashed line). Fractional changes in HO<sub>2</sub>, and in HO<sub>2</sub> + dNO/NO (solid lines).

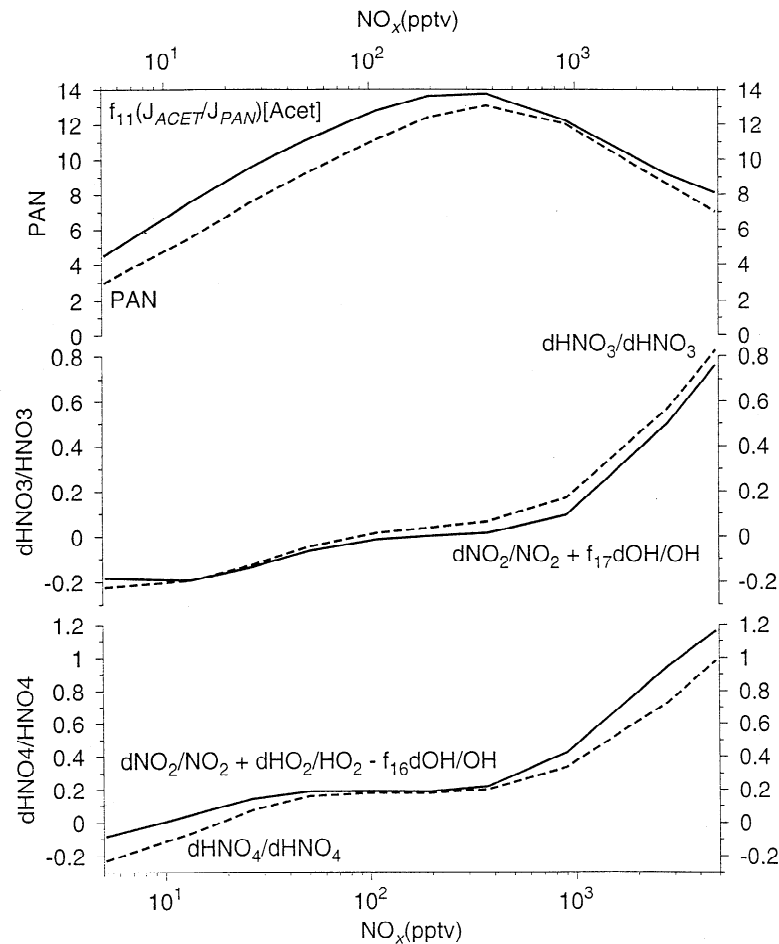


**Figure 9.** (bottom) The fractional change in HNO<sub>4</sub> from the introduction of acetone into the model (dotted line) compared with the change predicted by equation (16). (middle) The fractional change in HNO<sub>3</sub> from the introduction of acetone into the model (dotted line) compared with the change predicted by equation (17). (top) The change in peroxyacetylnitrate PAN from the introduction of acetone into the model (dotted line) compared with the change predicted by equation (19).

$$[dPAN] = f_{11} \frac{J_{ACET}}{J_{PAN}} [ACET]. \quad (19)$$

$$\frac{dNO}{NO} = -R \frac{dHO_2}{HO_2} - \frac{dPAN}{R_{bot}}. \quad (20)$$

The top panel of Figure 9 compares the concentration of PAN predicted by this expression with the PAN in the model. Despite the long lifetime of PAN in the upper troposphere, the agreement is again quite good. PAN increases of between 4 and 14 pptv in the upper tropical troposphere from acetone are comparable with three-dimensional model results [Singh *et al.*, 1995].

In Figure 10 the changes in PAN, HNO<sub>4</sub>, and HNO<sub>3</sub> from acetone have been normalized by the change in NO<sub>x</sub>. PAN reduces NO<sub>x</sub> most strongly at low NO<sub>x</sub>, where it not only absorbs all of the NO<sub>x</sub> decrease, but also lowers HNO<sub>4</sub> and HNO<sub>3</sub>. Conversion of NO<sub>x</sub> to HNO<sub>3</sub> dominates at large NO<sub>x</sub>. Conversion to HNO<sub>4</sub> is important for intermediate NO<sub>x</sub> mixing ratios.

If in (15) one substitutes (7) for  $dNO_2/NO_2$  (dropping the  $dO_3/O_3$  term because it proves to be unimportant), (16) for  $dHNO_4/HNO_4$ , (17) for  $dHNO_3/HNO_3$ , (19) for  $dPAN$ , and (5) for  $dOH/OH$ , one can write

The parameter  $R$  is given by

$$R = \quad (21)$$

$$\frac{f_{18}NO_2 + HNO_4(f_{18} + 1 - f_{16}) + HNO_3(f_{18} + f_{17})}{NO + NO_2 + HNO_4(1 - f_{16}f_{19}) + HNO_3(1 + f_{17}f_{19})}$$

$R$  helps estimate the decrease in NO from an increase in HO<sub>2</sub>, associated with increased conversions of NO to NO<sub>2</sub>, HNO<sub>3</sub>, and HNO<sub>4</sub> (but not PAN). It could be used to estimate the fractional decrease in NO, from a given increase in HO<sub>2</sub>, associated with a pure HO<sub>x</sub> source such as CH<sub>3</sub>OOH, which did not also produce PAN.

Figure 11 shows that  $R$  decreases steadily with NO<sub>x</sub>. Ozone production from a pure HO<sub>x</sub> source is therefore most heavily offset by decreases in NO at low NO<sub>x</sub>. The decrease in  $R$  with NO<sub>x</sub> is driven mainly by the decrease of  $f_{18}$  (shown in Figure 3).

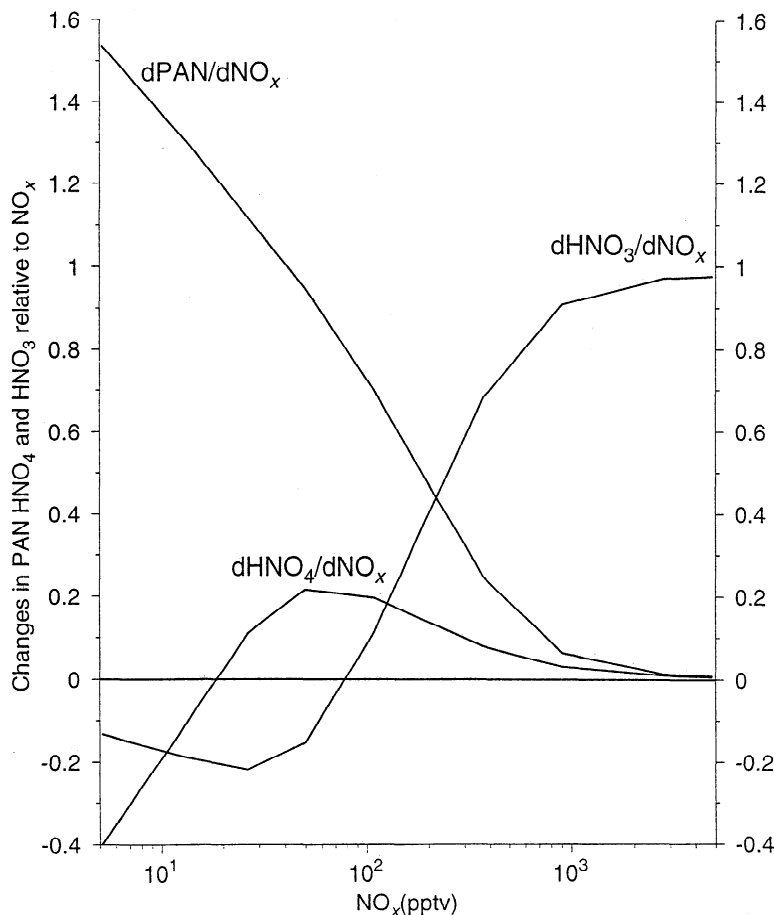


**Figure 10.** The changes in PAN, HNO<sub>4</sub>, and HNO<sub>3</sub> from the introduction of acetone, normalized by the absolute change in NO<sub>x</sub>.

The formation of PAN is also most effective at reducing ozone production at low NO<sub>x</sub>. The NO reduction caused by conversion of NO to PAN is accounted for by the second term on the right-hand side of (20). The parameter  $R_{bot}$  in (20) is simply the denominator of the right-hand side of (21). It is roughly proportional to

NO<sub>x</sub>. Since  $dPAN$  is only weakly dependent on NO<sub>x</sub> (Figure 9), the relative reductions in NO from PAN are largest at small NO<sub>x</sub>.

If one uses in (14) the expression for  $dNO/NO$  given by (20) and the expression for  $dPAN$  given in (19), the fractional change in  $P(O_3)$  is given by

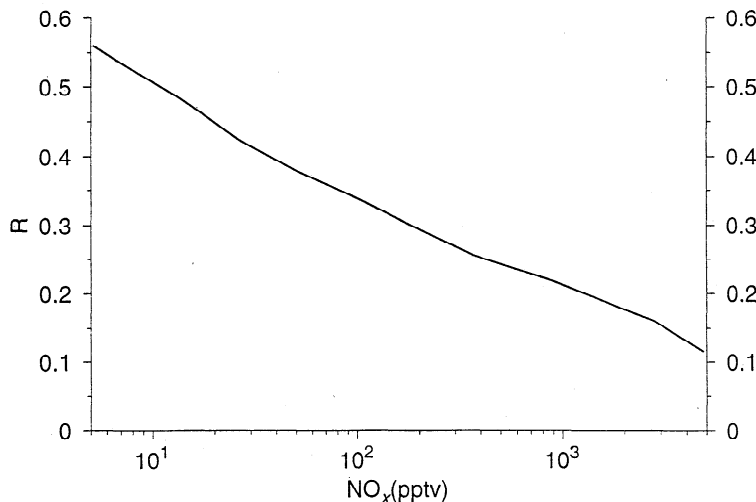


**Figure 11.** The variation with NO<sub>x</sub> of the HO<sub>x</sub>-NO<sub>x</sub> coupling coefficient  $R$  as defined by equation (21) in the text.

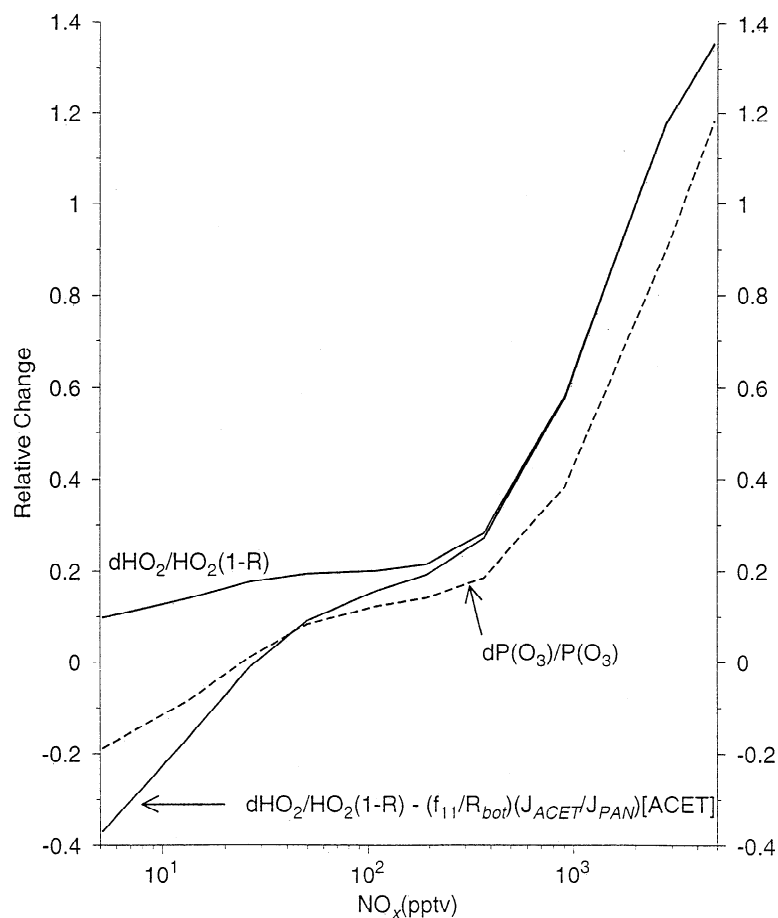


**Figure 12.** The fractional change in ozone production from adding acetone to the model (dashed line). The variation of  $d\text{HO}_2/\text{HO}_2(1+R)$  and the change in ozone production predicted by equation (22), plotted against  $\text{NO}_x$  (solid lines).

$$\frac{dP(\text{O}_3)}{P(\text{O}_3)} = \frac{d\text{HO}_2}{\text{HO}_2}(1-R) - \frac{f_{11}}{R_{\text{bot}}} \frac{J_{\text{acet}}}{J_{\text{PAN}}} [\text{ACET}]. \quad (22)$$

This expression gives an estimate for the change in ozone production from a given change in  $\text{HO}_2$  caused by acetone. For a  $\text{HO}_x$  source such as  $\text{CH}_3\text{OOH}$  that did not generate PAN, the second term on the right-hand side of (22) could be ignored. The two sides of (22) are compared in Figure 12. They agree reasonably well over a wide range of  $\text{NO}_x$  mixing ratios. The right-hand side of (22) underestimates ozone production at low  $\text{NO}_x$  because it overestimates PAN. The overestimate at high  $\text{NO}_x$  arises from the difference between  $dP(\text{O}_3)/P(\text{O}_3)$  and  $d\text{NO}/\text{NO} + d\text{HO}_2/\text{HO}_2$  shown in Figure 8. The right-hand side of (22) and  $d\text{HO}_2/\text{HO}_2(1-R)$  both converge exactly to  $d\text{HO}_2/\text{HO}_2 + d\text{NO}/\text{NO}$  in the high  $\text{NO}_x$  limit.

## 6. Summary

$\text{HO}_x$  sources such as acetone increase OH and  $\text{HO}_2$ . But the relative size of these increases is highly dependent on the  $\text{NO}_x$  concentration. They will increase rapidly with  $\text{NO}_x$  when  $\text{NO}_x$  concentrations become larger than 300 pptv. This is driven by decreases in

the strength of the other  $\text{HO}_x$  sources, by increases in the  $\text{HO}_x$  yield of acetone, and by changes in the chemistry of  $\text{HO}_x$  (self-buffered at low  $\text{NO}_x$  to  $\text{NO}_x$ -buffered at high  $\text{NO}_x$ ). Errors in our assessment of  $\text{HO}_x$  sources and sinks will therefore give rise to the largest relative errors in model estimates of OH and  $\text{HO}_2$  in the high  $\text{NO}_x$  regime. This may help account for a finding [Faloona *et al.*, 2000] that models tend to most strongly underestimate observed OH and  $\text{HO}_2$  concentrations at high  $\text{NO}_x$ .

Acetone will usually increase ozone production in the upper troposphere because it increases  $\text{HO}_2$ . But this increase will be substantially offset by reduced concentrations of NO. These are driven by complex interactions between the  $\text{HO}_x$  and  $\text{NO}_y$  families which favor the partitioning of  $\text{HO}_x$  toward  $\text{HO}_2$  and of  $\text{NO}_y$  from NO to more oxidized forms of nitrogen such as  $\text{NO}_2$ ,  $\text{HNO}_3$ ,  $\text{HNO}_4$ , and PAN. Much as with OH, the relative increase in ozone production from acetone will always increase with  $\text{NO}_x$ .

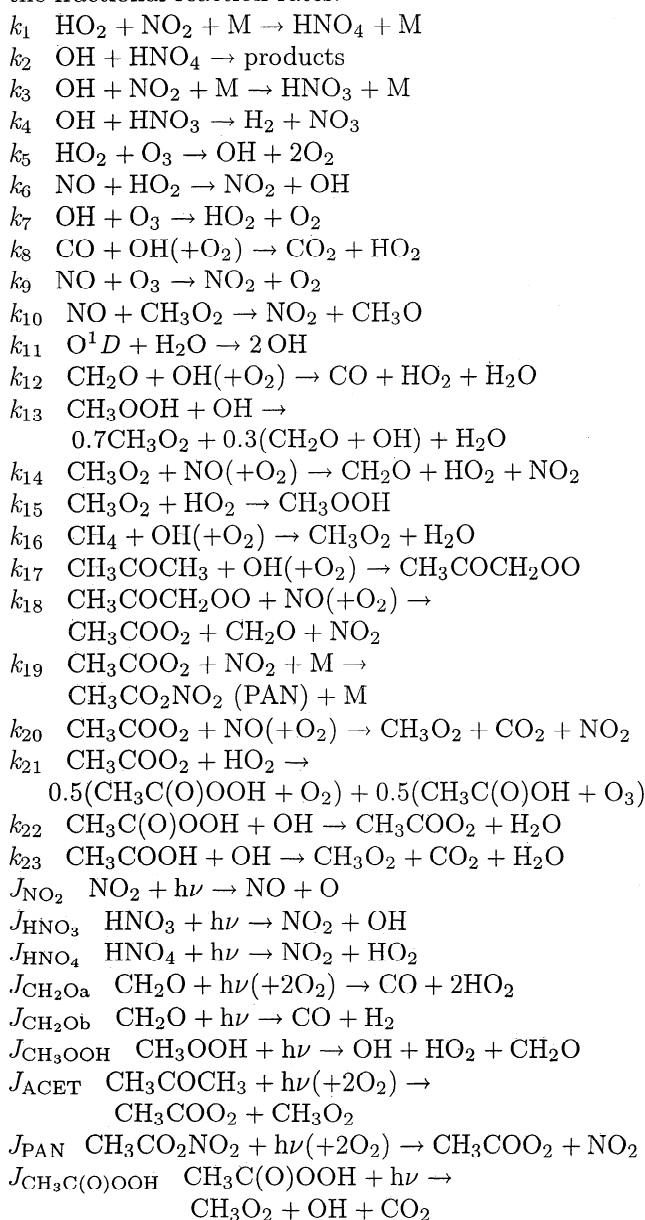
It should be kept in mind that although the relative increases in OH and ozone production from  $\text{HO}_x$  sources are largest in the high  $\text{NO}_x$  regime, the absolute increases in OH and ozone production from  $\text{HO}_x$  sources

will tend to be largest in the intermediate regime where OH and ozone production are maximized [Folkins et al., 1998].

Linear theory provides insight into some of the complex feedbacks that occur in the photochemistry of the atmosphere when it is subject to a perturbation such as a HO<sub>x</sub> source. There is nothing in this approach that restricts its applicability only to changes in the concentrations of HO<sub>x</sub> sources. It should therefore be useful in predicting the first-order chemical response of the atmosphere to the introduction of other trace species.

## Appendix A: Reaction Constants

This is a list of the reaction constants needed to define the fractional reaction rates.



## Appendix B: Fractional Reaction Rates

$$f_1 = J_{\text{CH}_2\text{Oa}} / (J_{\text{CH}_2\text{Oa}} + J_{\text{CH}_2\text{Ob}} + k_{12}[\text{OH}])$$

$$f_2 = J_{\text{CH}_2\text{Ob}} / (J_{\text{CH}_2\text{Oa}} + J_{\text{CH}_2\text{Ob}} + k_{12}[\text{OH}])$$

$$f_3 = k_{12}[\text{OH}] / (J_{\text{CH}_2\text{Oa}} + J_{\text{CH}_2\text{Ob}} + k_{12}[\text{OH}])$$

$$f_4 = J_{\text{CH}_3\text{OOH}} / (J_{\text{CH}_3\text{OOH}} + k_{13}[\text{OH}])$$

$$f_5 = k_{13}[\text{OH}] / (J_{\text{CH}_3\text{OOH}} + k_{13}[\text{OH}])$$

$$f_6 = k_{14}[\text{NO}] / (k_{15}[\text{HO}_2] + k_{14}[\text{NO}])$$

$$f_7 = k_{15}[\text{HO}_2] / (k_{15}[\text{HO}_2] + k_{14}[\text{NO}])$$

$$f_8 = J_{\text{ACET}} / (J_{\text{ACET}} + k_{17}[\text{OH}])$$

$$f_9 = k_{17}[\text{OH}] / (J_{\text{ACET}} + k_{17}[\text{OH}])$$

$$f_{10} = k_{20}[\text{NO}] / (k_{19}[\text{NO}_2] + k_{20}[\text{NO}] + k_{21}[\text{HO}_2])$$

$$f_{11} = k_{19}[\text{NO}_2] / (k_{19}[\text{NO}_2] + k_{20}[\text{NO}] + k_{21}[\text{HO}_2])$$

$$f_{12} = 0.5k_{21}[\text{HO}_2] / (k_{19}[\text{NO}_2] + k_{20}[\text{NO}] + k_{21}[\text{HO}_2])$$

$$f_{13} = f_{12}$$

$$f_{14} = k_{22}[\text{OH}] / (J_{\text{CH}_3\text{C(O)OOH}} + k_{22}[\text{OH}])$$

$$f_{15} = J_{\text{CH}_3\text{C(O)OOH}} / (J_{\text{CH}_3\text{C(O)OOH}} + k_{22}[\text{OH}])$$

$$f_{16} = k_2[\text{OH}] / (J_{\text{HNO}_4} + k_2[\text{OH}])$$

$$f_{17} = J_{\text{HNO}_3} / (J_{\text{HNO}_3} + k_4[\text{OH}])$$

$$f_{18} = k_6[\text{HO}_2] / (k_9[\text{O}_3] + k_6[\text{HO}_2])$$

$$f_{19} = k_6[\text{NO}] / (k_5[\text{O}_3] + k_6[\text{NO}])$$

## Appendix C: HO<sub>x</sub> Yield of Methane

An overview of methane oxidation is given in Figure 13. The main sink of CH<sub>4</sub> is OH attack. Although this reaction destroys one HO<sub>x</sub>, subsequent reactions almost invariably result in a net production of HO<sub>x</sub>. If HY(CH<sub>4</sub>) is the net number of HO<sub>x</sub> produced or destroyed during an OH-initiated oxidation of CH<sub>4</sub>, then the rate of HO<sub>x</sub> production from CH<sub>4</sub> oxidation can be written

$$\text{PHO}_x(\text{CH}_4) = k_{\text{OH}+\text{CH}_4}[\text{OH}][\text{CH}_4]\text{HY}(\text{CH}_4). \quad (\text{C1})$$

Since one HO<sub>x</sub> is used to produce CH<sub>3</sub>O<sub>2</sub> from CH<sub>4</sub>, the HO<sub>x</sub> yield of CH<sub>4</sub> can be simply related to the HO<sub>x</sub> yield of the methyl peroxy radical (CH<sub>3</sub>O<sub>2</sub>):

$$\text{HY}(\text{CH}_4) = \text{HY}(\text{CH}_3\text{O}_2) - 1. \quad (\text{C2})$$

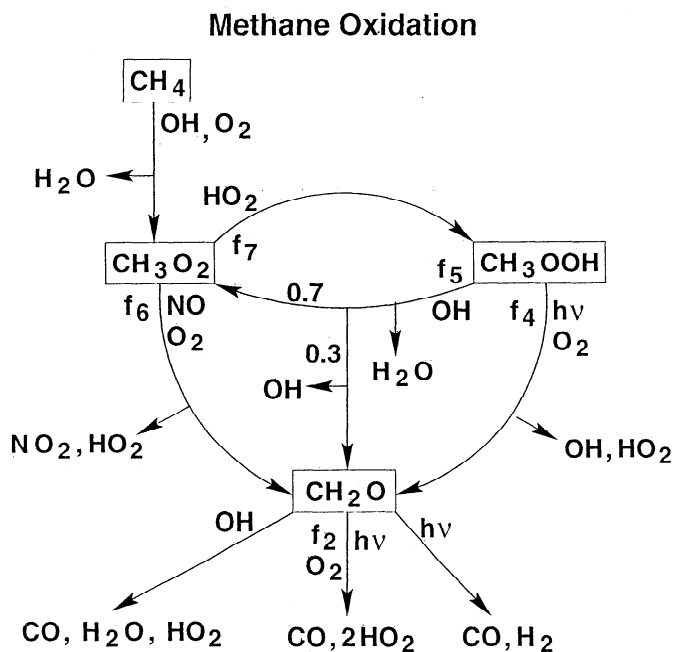


Figure 13. An overview of methane (CH<sub>4</sub>) oxidation.

CH<sub>3</sub>O<sub>2</sub> can react either with NO or HO<sub>2</sub>. Defining  $f_6$  and  $f_7$  as the fractional reaction rates for the two possibilities respectively, the HO<sub>x</sub> yield of CH<sub>3</sub>O<sub>2</sub> can be written

$$\text{HY}(\text{CH}_3\text{O}_2) = f_6[\text{HY}(\text{CH}_2\text{O}) + 1] + f_7[\text{HY}(\text{CH}_3\text{OOH}) - 1]. \quad (\text{C3})$$

The HO<sub>x</sub> yield of formaldehyde is simply

$$\text{HY}(\text{CH}_2\text{O}) = 2f_1, \quad (\text{C4})$$

where  $f_1$  is a fractional reaction rate for the photolysis of CH<sub>2</sub>O producing two HO<sub>2</sub>. The other two sinks of CH<sub>2</sub>O considered in Figure 13 are HO<sub>x</sub> neutral.

If  $f_4$  and  $f_5$  represent the fractional reaction rates of CH<sub>3</sub>OOH via photolysis and OH attack,

$$\text{HY}(\text{CH}_3\text{OOH}) = f_4[\text{HY}(\text{CH}_2\text{O}) + 2] + f_5[0.3\text{HY}(\text{CH}_2\text{O}) + 0.7\text{HY}(\text{CH}_3\text{O}_2) - 0.7] \quad (\text{C5})$$

The four constraints (C2) through (C5) can be used to solve for the HO<sub>x</sub> yields of CH<sub>4</sub>, CH<sub>2</sub>O, CH<sub>3</sub>O<sub>2</sub>, and CH<sub>3</sub>OOH. The HO<sub>x</sub> yield of CH<sub>3</sub>OOH is given by

$$\text{HY}(\text{CH}_3\text{OOH}) = \quad (\text{C6})$$

$$\frac{[2f_4(1 + f_1) + f_5(0.6f_1 - 0.7) + 0.7f_5f_6(1 + 2f_1) - 0.7f_5f_7]}{(1 - 0.7f_5f_7)}$$

The HO<sub>x</sub> yield of CH<sub>4</sub> can be obtained by using (C3), (C4), and (C6) in (C2).

## Appendix D: HO<sub>x</sub> Yield of Acetone

An overview of acetone oxidation is shown in Figure 14. The two major sinks of acetone are photolysis and OH attack. The rate of HO<sub>x</sub> production from acetone oxidation can be written

$$\text{PHO}_x(\text{ACET}) =$$

$$(J_{\text{ACET}} + k_{17}[\text{OH}])[\text{ACET}]\text{HY}(\text{ACET}). \quad (\text{D1})$$

If  $f_8$  and  $f_9$  represent the fractional reaction rates for photolysis and OH attack,

$$\text{HY}(\text{ACET}) = f_8(\text{HY}(\text{CH}_3\text{O}_2) + \text{HY}(\text{CH}_3\text{COO}_2)) + f_9(\text{HY}(\text{CH}_2\text{O}) + \text{HY}(\text{CH}_3\text{COO}_2) - 1). \quad (\text{D2})$$

Appendix C shows how to evaluate HY(CH<sub>3</sub>O<sub>2</sub>) and HY(CH<sub>2</sub>O). We assume PAN is stable. Use PAA (peracetic acid) to denote CH<sub>3</sub>C(O)OOH and AA (acetic acid) to denote CH<sub>3</sub>C(O)OH. The HO<sub>x</sub> yield of the CH<sub>3</sub>COO<sub>2</sub> radical is given by

$$\text{HY}(\text{CH}_3\text{COO}_2) = f_{10}\text{HY}(\text{CH}_3\text{O}_2) + f_{12}(\text{HY}(\text{PAA}) - 1) + f_{13}(\text{HY}(\text{AA}) - 1). \quad (\text{D3})$$

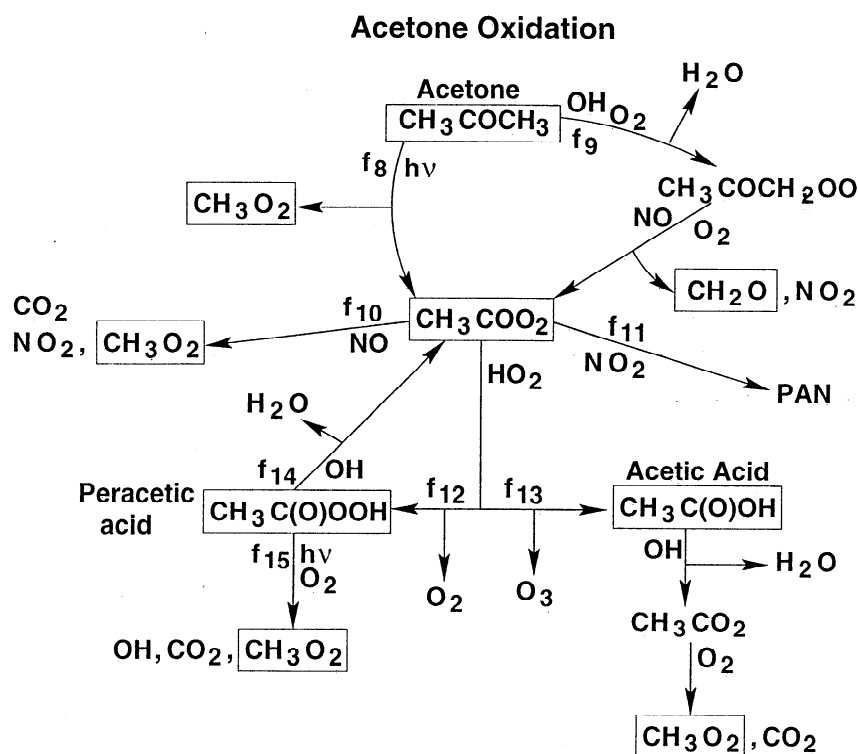


**Figure 14.** An overview of acetone (CH<sub>3</sub>COCH<sub>3</sub>) oxidation. One simplification has been to ignore the reaction of CH<sub>3</sub>COCH<sub>2</sub>O<sub>2</sub> with HO<sub>2</sub>. There is little kinetic information available on this reaction, but it can be estimated to be competitive with the NO reaction only for NO ≤ 20 pptv.

The HO<sub>x</sub> yield of PAA can be written

$$\begin{aligned} \text{HY(PAA)} &= f_{14}(\text{HY}(\text{CH}_2\text{COO}_2) - 1) \\ &+ f_{15}(\text{HY}(\text{CH}_3\text{O}_2) + 1). \end{aligned} \quad (\text{D4})$$

The HO<sub>x</sub> yield of AA can be written

$$\text{HY(AA)} = \text{HY}(\text{CH}_3\text{O}_2) - 1. \quad (\text{D5})$$

These equations can be used to show that

$$\begin{aligned} \text{HY}(\text{CH}_3\text{COO}_2) &= \\ \frac{[\text{HY}(\text{CH}_3\text{O}_2)(f_{10} - f_{12}f_{15} + f_{13}) - 2f_{13}]}{(1 - f_{12}f_{14})}. \end{aligned} \quad (\text{D6})$$

The HO<sub>x</sub> yield of acetone can then be determined by using (D6) and the known HO<sub>x</sub> yields of CH<sub>3</sub>O<sub>2</sub> and CH<sub>2</sub>O in (D2).

**Acknowledgments.** This research was supported by the Natural Sciences and Engineering Council of Canada. R. Chatfield acknowledges the support of grant 622-61-10-10 from NASA's Global Tropospheric Experiment, with model development aided by the Modeling and Analysis Program, grant 622-59-39-10.

## References

- Arnold, F., V. Burger, B. Droste-Fanke, F. Grimm, A. Krieger, J. Schneider, and T. Stilp, Acetone in the upper troposphere and lower stratosphere: Impact on trace gases and aerosols, *Geophys. Res. Lett.*, *24*, 3017-3020, 1997.
- Chatfield, R. B., and P. J. Crutzen, Sulfur dioxide in remote oceanic air: Cloud transport of reactive precursors, *J. Geophys. Res.*, *89*, 7111-7132, 1984.
- Chatfield, R. B., J. A. Vastano, H. B. Singh, and G. Sachse, A general model of how fire emissions and chemistry produce African/oceanic plumes (O<sub>3</sub>, CO, PAN, smoke) in TRACE A, *J. Geophys. Res.*, *101*, 24,279-24,306, 1996.
- Faloona, I., et al., Observations of HO<sub>x</sub> and its relationship with NO<sub>x</sub> in the upper troposphere during SONEX, accepted in *J. Geophys. Res.*, *105*, 3771-3783, 2000.
- Folkins, I., P. O. Wennberg, T. F. Hanisco, J. G. Anderson, and R. J. Salawitch, OH, HO<sub>2</sub>, and NO in two biomass burning plumes: Sources of HO<sub>x</sub> and implications for ozone production, *Geophys. Res. Lett.*, *24*, 3185-3188, 1997.
- Folkins, I. A., R. Chatfield, H. Singh, Y. Chen, and B. Heikes, Ozone production efficiencies of acetone and peroxides in the upper troposphere, *Geophys. Res. Lett.*, *25*, 1305-1308, 1998.
- Jacob, D. J., et al., Origin of ozone and NO<sub>x</sub> in the tropical troposphere: A photochemical analysis of aircraft observations over the South Atlantic basin, *J. Geophys. Res.*, *101*, 24,235-24,250, 1996.
- Jaeglé, L., et al., Observed OH and HO<sub>2</sub> in the upper troposphere suggest a major source from convective injection of peroxides, *Geophys. Res. Lett.*, *24*, 3181-3184, 1997.
- Jaeglé, L., D. J. Jacob, Y. Wang, A. J. Weinheimer, B. A. Ridley, T. L. Campos, G. W. Sachse, and D. E. Hagen, Sources and chemistry of HO<sub>x</sub> in the upper troposphere over the United States, *Geophys. Res. Lett.*, *25*, 1705-1708, 1998.
- Keim, E. R. et al., NO<sub>y</sub> partitioning from measurements of nitrogen and hydrogen radicals in the upper troposphere, *Geophys. Res. Lett.*, *26*, 51-54, 1999.
- McKeen, S. A., T. Gierczak, J. B. Burkholder, P. O. Wennberg, T. F. Hanisco, E. R. Keim, R.-S. Gao, S. C. Liu, A. R. Ravishankara, and D. W. Fahey, The photochemistry of acetone in the upper troposphere: A source of odd-hydrogen radicals, *Geophys. Res. Lett.*, *24*, 3177-3180, 1997.
- Müller, J. F., and C. Brasseur, Sources of upper tropospheric HO<sub>x</sub>: A three-dimensional study, *J. Geophys. Res.*, *104*, 1705-1715, 1999.
- Prather, M. J., and D. J. Jacob, A persistent imbalance in HO<sub>x</sub> and NO<sub>x</sub> photochemistry of the upper troposphere driven by deep tropical convection, *Geophys. Res. Lett.*, *24*, 3189-3192, 1997.
- Singh, H. B., M. Kanakidou, P. J. Crutzen, and D. J. Jacob, High concentration and photochemical fate of oxygenated hydrocarbons in the global troposphere, *Nature*, *378*, 50-54, 1995.
- Wennberg, P. O., et al., Hydrogen radicals, nitrogen radicals, and the production of ozone in the upper troposphere, *Science*, *279*, 49-53, 1998.

R. Chatfield, Earth Science Division, NASA Ames Research Center, MS 245-5, Moffett Field, CA 94035. (chatfield@clio.arc.nasa.gov)

I. Folkins, Department of Oceanography, Dalhousie University, Halifax, Nova Scotia, Canada B3H 4J1. (Ian.Folkins@dal.ca)

(Received October 22, 1999; revised January 20, 2000; accepted January 27, 2000.)